Yeast Resolving Enzyme CCE1 Makes Sequential Cleavages in DNA Junctions within the Lifetime of the Complex[†]

Jonathan M. Fogg, Mark J. Schofield, Anne-Cécile Déclais, and David M. J. Lilley*

CRC Nucleic Acid Structure Research Group, Department of Biochemistry, The University of Dundee, Dundee DD1 4HN, U.K.

Received December 6, 1999; Revised Manuscript Received January 20, 2000

ABSTRACT: CCE1 is a DNA junction-resolving enzyme of *Saccharomyces cerevisiae*. Such enzymes are required to make two symmetrically paired cleavages in order to resolve the four-way junction productively. Using a cruciform assay, we show here that CCE1 introduces two unilateral cleavages in a sequential manner. This requires that the protein remains bound to the junction, preventing branch migration of the point of strand exchange. From a detailed kinetic analysis, we find that the CCE1 cleavage at a given site is accelerated by a factor of 5−10 when it occurs subsequently to the initial cleavage. These properties ensure a productive resolution of the four-way junction and may be general for junction-resolving enzymes.

The four-way junction is the central intermediate in homologous recombination (*1*−*5*), and the manner of its resolution can determine the genetic outcome of the process. Resolution into discrete duplex species is brought about by a class of structure-selective nucleases, the junction-resolving enzymes (*6*). These proteins have been isolated from bacteriophage-infected *Escherichia coli* (*7*, *8*), eubacteria (*9*, *10*), yeast (*11*−*13*), mammals (*14*), and their viruses (*15*).

Productive resolution of a four-way DNA junction requires the hydrolysis of two symmetrically disposed phosphodiester bonds. Departure from this symmetry will result in the formation of nicked species, and an unproductive resolution event. All junction-resolving enzymes isolated to date bind to four-way junctions in dimeric form, and thus the required cleavages are catalyzed by individual protomers. This creates a potential problem in terms of ensuring the required paired bilateral cleavage, particularly in the context of a junction that can be repositioned by branch migration. This could be especially acute for enzymes that exhibit sequence specificity at the level of cleavage, such as yeast CCE1 (*16*, *17*) and RuvC of *E. coli* (*18*, *19*), where a range of kinetic rates of cleavage is possible. The importance of achieving productive resolution suggests that some molecular mechanism might be required to ensure it.

We have previously devised a procedure for analyzing the temporal order of cleavages in a four-way junction, based on a cruciform maintained in a negatively supercoiled plasmid (*20*). In earlier experiments we showed that the phage junction-resolving enzymes T4 endonuclease VII and T7 endonuclease I resolved such plasmids into linear products. There are two explanations for such a result, illustrated schematically in Figure 1. First, the cleavages could occur simultaneously via a coordination between the activities of the two subunits. Second, one site could be cleaved unilaterally, in which case the existence of the extruded cruciform would have to be preserved by the binding of the protein, thus preventing reabsorption into the nicked plasmid and permitting subsequent cleavage at the second site.

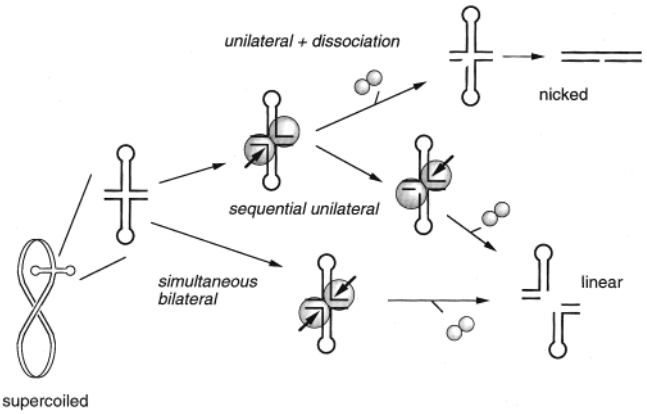

FIGURE 1: Schematic to illustrate the possible products of resolution of a supercoil-stabilized cruciform structure. The cruciform structure formed by extrusion of an inverted repeat is stable only in a supercoiled DNA molecule. If this is resolved by simultaneous bilateral cleavage by a resolving enzyme, the result is a linear DNA species. Unilateral cleavage would be expected to release the superhelical constraint and, thus, destabilize the cruciform which would thereby be reabsorbed. If this occurs, no further cleavage is possible and the result is a nicked circular DNA species. However, if the nicked junction is tightly held by the enzyme such that the structure is preserved, a second cleavage might be possible, leading to a linear product. Thus linear product could be generated either by simultaneous bilateral cleavage, or sequential unilateral cleavage with protein-mediated preservation of structure.

In the present study, we have made a kinetic analysis of the cleavage events induced by the junction-resolving enzyme CCE1 of *Saccharomyces cerevisiae*. This is a nuclear-encoded mitochondrial enzyme (*21*−*23*). Like other resolving enzymes, it binds to four-way DNA junctions as a dimer and introduces two cleavages at the point of strand exchange (*16*). In addition, CCE1 exhibits a marked sequence preference at the level of the phosphodiesterase reaction (*16*, *17*). Using the cruciform-cleavage assay, we have observed the

[†] This work was supported by the Cancer Research Campaign.

* To whom correspondence should be addressed. Phone: (44)-1382-344243. Fax: (44)-1382-201063. E-mail: dmjlilley@bad.dundee.ac.uk.

10.1021/bi992785v CCC: $19.00
Published on Web 03/16/2000

transient formation of a nicked intermediate in the cleavage reaction, demonstrating that the process occurs via two sequential, unilateral cleavages. Detailed analysis of the kinetics of the reactions reveals that the cleavage at a given site is accelerated by a factor of 5−10 when it occurs subsequently to the initial cleavage, thereby facilitating productive paired resolution cleavages. This indicates a close interaction between cleavage events and the structure of the DNA junction.

RESULTS

Principle of the Cruciform Assay. We have previously used a supercoil-stabilized cruciform structure as a self-limiting substrate (*20*), illustrated in Figure 1. Cruciform structures are formed by intrastrand base pairing in inverted repeat sequences in DNA and consist of a pair of hairpin loops extruded from the DNA (*24*−*26*). The region at the base of these stem loops is a four-way junction that can act as a substrate for Holliday junction-resolving enzymes (*27*, *28*). Cruciform structures have significantly positive free energies of formation in linear DNA (*26*, *29*−*31*). They only enjoy a stable existence in negatively supercoiled DNA, where the free energy is supplied by the local unwinding of the DNA which leads to partial relaxation of supercoiling. For this reason, the cruciform only exists while the DNA remains supercoiled, and any break introduced in the DNA will release the supercoiling and thus destabilize the cruciform leading to its reabsorption into duplex DNA. This is the key to the principle of this experiment. If the enzyme introduces a unilateral cleavage into the junction such that the topological constraint of the molecule is released, the cruciform will disappear and no further reaction should be possible. Under these circumstances, the product of the reaction will be nicked-circular DNA. On the other hand, if the enzyme were to coordinate the cleavages at both sites in the junction, the product would be linear DNA. Since these products are readily separated by agarose gel electrophoresis, it is straightforward to distinguish these alternative outcomes.

Construction of a Cruciform-Extruding Sequence with CCE1 Cleavage Sites. To examine the relationship between the two phosphodiester cleavages in the resolution of a four-way junction by the subunits of CCE1, we required a plasmid containing a cruciform stabilized by negative supercoiling. The design of such a cruciform was constrained by two requirements for cleavage by CCE1. First, the enzyme cleaves most efficiently at the point of strand exchange in a four-way junction (*17*). Second, CCE1 exhibits marked sequence preference for cleavage, with the most rapidly cleaved sequence being ACT↓A (where ↓ denotes the position of cleavage) (*16*, *17*). To ensure that the cleavage site is located at the point of strand exchange, the extrusion of the cruciform must halt at this point, and thus the 2-fold symmetry of the inverted repeat must terminate after the T that is 5′ to the cleavage. To prevent further branch migration, the two CCE1 sites must therefore differ in sequence at the position 3′ to the cleavage point, and we therefore used the second-fastest cleavage sequence ACT↓G (*17*). The sequence of the cruciform is shown in linear form in Figure 2A and as a cruciform in Figure 2B. The central part of the inverted repeat, including the loops of the cruciform, comprised an alternating adenine-thymine sequence; this results in rapid extrusion kinetics (*31*, *32*) and, thus, facilitates formation of the cruciform experimentally. The two cleavage sites will be subsequently referred to as site A (i.e., the site of sequence ACTA) and site G (sequence ACTG).

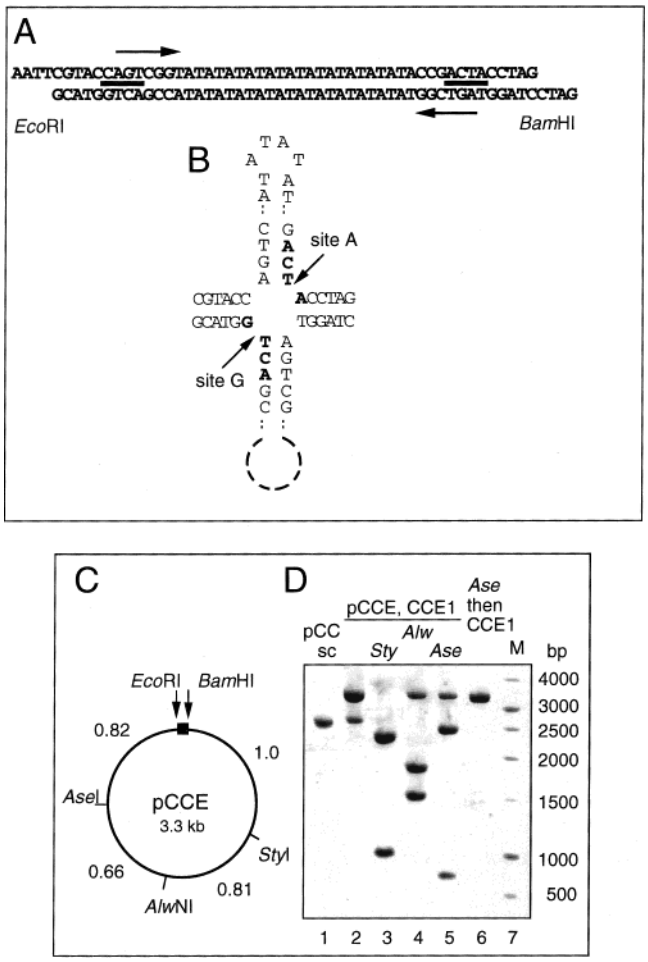

FIGURE 2: CCE1-cleavable cruciform of pCCE. (A) The sequence of the inverted repeat. The sequence between the two arrows has 2-fold symmetry, and can form a perfect cruciform structure. The sections indicated by solid bars are the ACTA and ACTG targets for CCE1 cleavage. The middle section of the cruciform consists of alternating adenine-thymine sequence, which undergoes cruciform extrusion with minimal kinetic barrier. (B) The inverted repeat drawn as a cruciform. The CCE1 target sequences are indicated in bold, and the two cleavage sites indicated by the arrows. The sites are named site A (ACTA) and site G (ACTG) as shown. (C) A circular map of pCCE, showing a number of restriction sites used in the characterization of the plasmid. The distances between sites are indicated (kbp). (D) Characterization of pCCE. Supercoiled pCCE DNA is shown in track 1. Following incubation with CCE1, the DNA is substantially converted to the linear species (track 2). When this CCE1-generated linear DNA was subsequently cleaved to completion by unique-site restriction enzymes *Sty*I, *Alw*NI, and *Ase*I (tracks 3−5, respectively), two linear subfragments were generated in each case. The sizes of these fragments were estimated using a semilogarithmic plot of mobilities against known sizes of marker DNA fragments (track 7; lengths given on right), giving values of 2.4 (2.3) and 0.9 (1.0) kbp for *Sty*I, 1.9 (1.8) and 1.5 (1.5) kbp for *Alw*NI and 2.5 (2.5) and 0.8 (0.8) kbp for *Ase*I, where the values in parentheses have been calculated, based on the assumption of CCE1 cleavage at the cruciform structure. Track 6 contains pCCE that was linearized with *Ase*I and then incubated with CCE1.

The plasmid pCCE (Figure 2C) containing the required inverted repeat was constructed by ligation of synthetic oligonucleotides between the *Bam*HI and *Eco*RI restriction sites of pAT153. Supercoiled plasmid was prepared by 2-fold

isopycnic centrifugation in order to have a high proportion of covalently closed circular DNA. Cleavage of the supercoiled DNA with CCE1 resulted in linearization of the DNA (Figure 2D, track 2); by contrast a plasmid containing a similar inverted repeat lacking the CCE1 cleavage sequence was not cleaved (data not shown). When pCCE was first linearized by cleavage with *Ase*I, followed by incubation with CCE1, no cleavage by the resolving enzyme was observed because the cruciform had been reabsorbed in the linear DNA (Figure 2D, track 6). The position of CCE1 cleavage of supercoiled pCCE was analyzed by restriction cleavage of CCE1-linearized plasmid (Figure 2D, tracks 3−5), using the enzymes *Sty*I, *Alw*NI, and *Ase*I for which single sites exist in pCCE. The lengths of the DNA fragments generated were fully consistent with cleavage at the inverted repeat sequence.

Bilateral Cleavage of a Cruciform by CCE1. pCCE was used to analyze the timing between the cleavages induced in a four-way junction by CCE1 resolving enzyme. Supercoiled pCCE DNA was incubated with increasing amounts of CCE1 at 37 °C for 5 min, and the reaction terminated by addition of EDTA. Uncleaved supercoiled substrate and the two potential products were separated by electrophoresis in an agarose gel (Figure 3A). Incubation with increasing concentrations of CCE1 resulted in a loss of supercoiled substrate DNA, with a corresponding appearance of linear (form III) plasmid. The very small fraction of open-circular DNA was essentially unchanged during the reaction. This is similar to previous results with bacteriophage junction-resolving enzymes (*20*, *33*) and indicates that the junction of the cruciform undergoes bilateral cleavage during the lifetime of the protein−junction complex. The experiment was repeated using a shorter incubation time of 1 min (data not shown). Under these conditions, we observed the generation of both linear and open-circular products. The latter must result from unilateral cleavage of the cruciform by CCE1 and, therefore, indicates that the two cleavages are not necessarily simultaneous. This is explored further below.

Independent Cleavage Activity of CCE1 Subunits. To generate linear product, two CCE1 cleavages must occur within the lifetime of the junction−enzyme complex. Dissociation of the complex after the first cleavage would leave a nicked plasmid that is no longer supercoiled, whereupon the cruciform would be reabsorbed and, thus, no further cleavage would occur. One possible way of ensuring bilateral cleavage might be to link the two cleavages in some manner, such that cleavage could not occur at one site without a cleavage reaction at the opposing site. However, the formation of an open-circular intermediate at short incubation times suggests that the two cleavages occur independently.

To test this further, we carried out an experiment designed to generate a heterodimer of CCE1 containing one active and one inactive subunit. In this way, we could see whether the active subunit can still function in cleavage of the DNA junction in a situation where its partner subunit is inactive. For this purpose, we used a mutant form of CCE1, D294N, which binds normally to four-way DNA junctions but is completely inactive in cleavage (M. F. White and D.M.J.L., unpublished data). CCE1 readily undergoes subunit exchange in free solution (*16*), and therefore heterodimers containing one active and one inactive subunit can be formed by simple mixing.

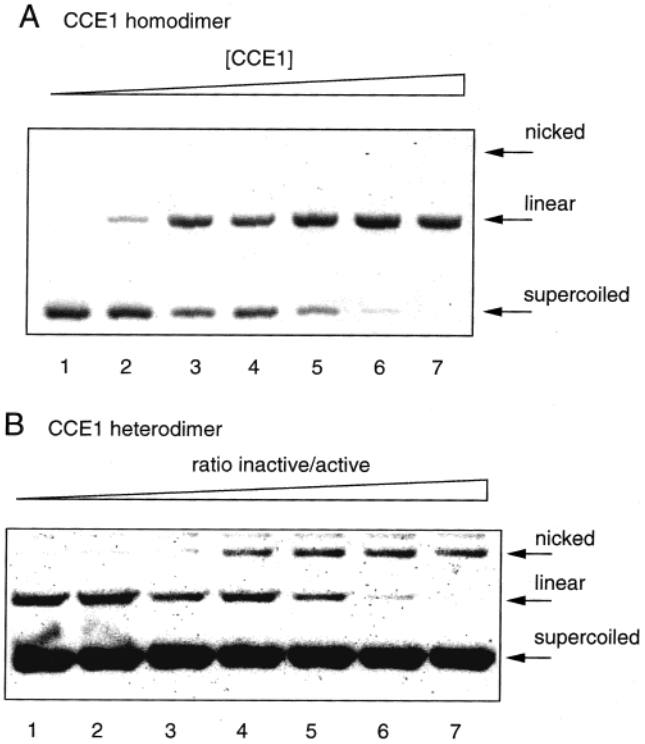

FIGURE 3: Cleavage of supercoiled pCCE with increasing concentrations of CCE1. For both experiments, 20 nM supercoiled pCCE was incubated with CCE1 at 37 °C for a fixed time. The reaction was terminated using EDTA, and after deproteinisation the products were separated by electrophoresis in an agarose gel in order to resolve the nicked, linear and supercoiled plasmid (indicated right). Gels were stained using ethidium bromide, and DNA species visualized by fluorography. (A) Formation of linear DNA by active CCE1. pCCE was incubated with increasing concentrations of wild-type CCE1 for 5 min. Under these conditions, the supercoiled DNA disappears and linear product appears with increasing digestion by CCE1; nicked pCCE is not discernible in this experiment. The concentrations of CCE1 used were 63, 125, 250, 500 nM, 1, 2, and 4 μM in tracks 1−7, respectively. (B) Formation of nicked DNA by an active-inactive heterodimer of CCE1. A fixed concentration of wild-type CCE1 (100 nM) was mixed with an increasing concentration of inactive D294N CCE1 to generate the molar ratios given below. pCCE was incubated with the mixtures of wild-type and inactive CCE1 for 10 min. While at low molar ratios of inactive CCE1, the product is linear DNA, as the mole fraction of inactive CCE1 increases an increasing proportion of nicked product results. Evidently the active-inactive heterodimer of CCE1 generates unilaterally cleaved DNA, indicating that an active CCE1 protomer can function in combination with an inactive subunit. The molar ratios of active/inactive CCE1 were 0.5, 1, 2, 4, 6, 8, and 10 in tracks 1−7, respectively.

We incubated supercoiled pCCE with an increasing concentration of catalytically inactive D294N CCE1 in the presence of a fixed concentration of wild-type, active CCE1 (Figure 3B). When the ratio of active to inactive protein was high, the product of the reaction was linear DNA. However, as the molar ratio of inactive protein increased, the fraction of open circular product increased. Thus, as the extent of active-inactive heterodimer increased, the cruciform became subject to unilateral cleavage. The proportion of inactive protein required to observe nicked product was higher than that expected theoretically, and might indicate incomplete subunit mixing. Nevertheless, the qualitative result is clear. Clearly, the active subunit can function when paired with an inactive protomer and, therefore, does not require an active partner subunit for activity.

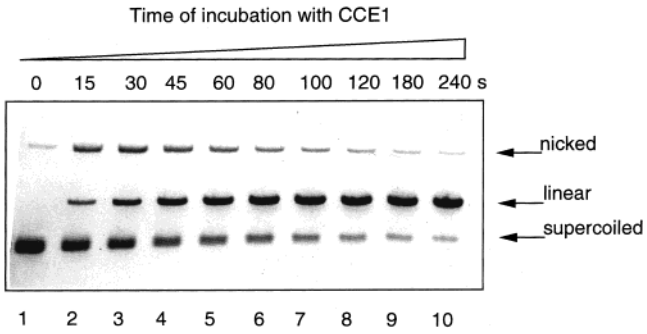

FIGURE 4: Cleavage of pCCE with CCE1 as a function of time. Supercoiled pCCE (20 nM) was incubated with 1 μM CCE1 at 37 °C. Aliquots were removed after increasing lengths of time, and the reaction was terminated. After deproteinization, the products were separated by electrophoresis in an agarose gel in order to resolve the nicked, linear and supercoiled plasmid (indicated right). It is apparent that nicked DNA is generated as a transient intermediate at the shorter time intervals. The gel was stained using ethidium bromide, and DNA species visualized by fluorography. The times of reaction were 0, 15, 30, 45, 60, 80, 100, 120, 180, and 240 s in tracks 1−10, respectively.

The outcome of this experiment also confirms the basic premise of this experiment. The absence of linear product under these conditions shows that the nicked cruciform cannot survive the dissociation of the heterodimer CCE1, since the binding of an oppositely oriented dimer to generate the second cleavage is evidently not observed.

Sequential Cleavage Reactions by CCE1 Subunits. The formation of open-circular plasmid at short times of incubation with CCE1 suggests that the two cleavages do not occur simultaneously. To investigate this further, we studied the cleavage of pCCE with a fixed concentration of CCE1 as a function of time under single turnover conditions (Figure 4). We find that at early times the product is mainly open-circular DNA, indicative of unilateral cleavage. The proportion of this species was maximal within the first minute of incubation, after which it slowly disappeared. The initial rate of appearance of the open-circular species was approximately equal to the rate of disappearance of supercoiled substrate. With increasing time, the amount of linear product increased at a rate approximately equal to the subsequent disappearance of the open circular species. Linear product was still being generated even after the supercoiled substrate was almost completely digested. This indicates that the open circular intermediate is a substrate for the formation of linear DNA and that the junction is, therefore, being held in the correct conformation for cleavage in the complex with the enzyme. A kinetic analysis of the formation of the different products is given below.

Relative Extent of Cleavage at the Two CCE1 Sites. In principle, open-circular DNA could result from one of two possible unilateral cleavage events, at either site A or G. We, therefore, examined the relative extent of cleavage at the two sites in the open-circular DNA. The band containing this product of CCE1 cleavage was excised from the gel, and the DNA recovered by electroelution. After radioactive 5′-^{32}P-labeling, the DNA was cleaved with *Ssp*I and *Sph*I restriction enzymes at sites flanking the inverted repeat sequence, and the labeled DNA separated by gel electrophoresis (Figure 5). It was observed that there was a significant preference for cleavage at the site A (ACTA sequence) rather than site G (ACTG) (a ratio of 1.9:1 at 30 s. determined by phosphorimaging, assuming equal efficiencies of phosphorylation for the two termini generated by CCE1), consistent with the findings of Schofield et al. (*17*) showing that ACTA was cleaved faster by CCE1 than ACTG in isolated junctions. The bias in cleavage frequencies is determined by the efficiencies with which the sites are cleaved by CCE1, and this is discussed further below. The corresponding experiment on the linear product gave two bands of equal intensity, indicating that the two ends generated by CCE1 are phosphorylated with equal efficiency.

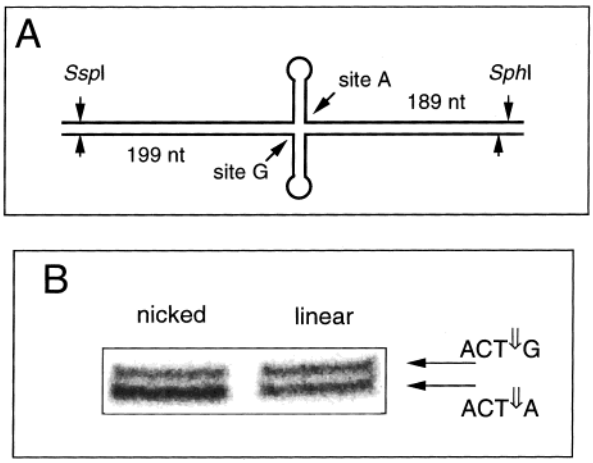

FIGURE 5: Ratio of nicked intermediates in CCE1 cleavage. The nicked transient apparent in the shorter time courses of CCE1 cleavage (Figure 4) would be expected to contain DNA that had been cleaved at either site A or site G. To quantify these cleavages separately, the nicked DNA from a 30 s. incubation with CCE1 was recovered from agarose by electroelution and subjected to restriction analysis. (A) The principle of the experiment. pCCE was incubated with CCE1 and the nicked and linear species separated electrophoretically and purified. The resulting 5′-termini were radioactively ^{32}P-labeled, and the DNA then subjected to complete digestion by a mixture of the restriction enzymes *Ssp*I and *Sph*I. Cleavage at site A should generate a single-stranded DNA species of 189 nt in length, while cleavage at site G should generate a fragment of 199 nt. The products were separated on a sequencing polyacrylamide gel, and the radioactive fragments visualized and quantified by phosphorimaging. (B) Phosphorimage showing the products resulting from restriction cleavage of nicked and linear species. While the linear species results in two fragments of closely similar radioactivity, those resulting from the nicked DNA exhibit a 1.9:1 ratio in favor of cleavage at site A.

Transient Formation of Open-Circular DNA by T7 Endonuclease I. It has been shown previously that the phage enzymes T4 endonuclease VII (*20*) and T7 endonuclease I (*33*) cleave junctions bilaterally within the lifetime of the junction−enzyme complex. In light of the results using CCE1, we may ask whether we can detect nicked intermediates in the resolution of cruciform junctions by resolving enzymes of phage origin. The choice of cruciform sequence is relatively unimportant for phage enzymes, which exhibit very much lower sequence selectivity for cleavage. We therefore incubated supercoiled pCCE with a fixed concentration of T7 endonuclease I, and followed the progress of the reaction as a function of time. Since this enzyme is intrinsically faster than CCE1, the incubation was performed at 4 °C in order to slow the cleavage reaction. The products were analyzed by gel electrophoresis as before (Figure 6). Even at this relatively low temperature, a rapid digestion of supercoiled substrate was observed. As with CCE1, there was a transient formation of open-circular DNA followed

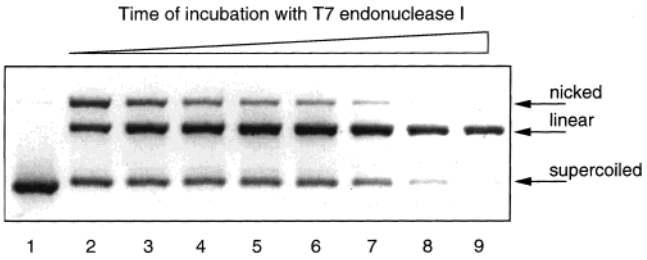

FIGURE 6: Cleavage of pCCE with T7 endonuclease I as a function of time. Supercoiled pCCE (40 nM) was incubated with 1 μM T7 endonuclease I at 4 °C. Aliquots were removed after increasing lengths of time, and the reaction was terminated. After deproteinization, the products were separated by electrophoresis in an agarose gel in order to resolve the nicked, linear, and supercoiled plasmid (indicated right). As with CCE1, it is clear that nicked DNA is generated as a transient intermediate at the short times. The gel was stained using ethidium bromide, and DNA species visualized by fluorography. The times of reaction were 0, 10, 20, 30, 40, 50, 60, 90, and 120 s in tracks 1−9, respectively.

by conversion to the final linear product. This indicates that the bound protein supports the structure of the junction, thus preventing the reabsorption of the nicked cruciform, and suggests that this may be general for the junction-resolving enzymes.

DISCUSSION

Using a supercoil-stabilized cruciform structure that contains CCE1 target sequences, we have shown that the yeast junction-resolving enzyme CCE1 introduces bilateral cleavages into the junction during the lifetime of the DNA−protein complex. Thus, after extended incubation with CCE1 enzyme, supercoiled pCCE plasmid becomes fully converted to linear product. Enzyme-free, unilaterally cleaved DNA would be topologically unconstrained, and the cruciform would be rapidly reabsorbed, thus, removing the substrate and preventing a second cleavage that could linearize the DNA; indeed this is exactly the result of the experiment using heterodimeric active/inactive CCE1. The conversion to linear DNA by fully active CCE1, therefore, indicates that both cleavages must occur without dissociation of the enzyme−junction complex. Corresponding behavior has previously been observed for the sequence-independent phage resolving enzymes, T4 endonuclease VII (*20*), and T7 endonuclease I (*33*).

Our new results clearly demonstrate that the two cleavages induced in the junction by CCE1 occur independently. They are not necessarily simultaneous, but are in general sequential. However, following the first cleavage on either side, the resulting nicked junction does not result in the reabsorption of the cruciform, because the junction is still available for the second cleavage which proceeds quantitatively. By contrast, when an active/inactive heterodimer of CCE1 was used, the nicked product was generated, showing that the cruciform junction could not survive dissociation and reassociation of enzyme. Thus, the complex of CCE1 with the DNA maintains the physical integrity of the four-way junction. Previous measurements have shown that the free energy of cruciform formation is generally of the order of 14−18 kcal mol^{-1} (*26, 29−31*), and thus the binding of the resolving enzyme is required to provide a considerable stabilization of the structure in the absence of topological constraint. Furthermore, the complex must be stable over a relatively long period; we have seen that the nicked intermediate species can be quite long-lived, with a lifetime in the range of minutes.

The sequential cleavage process observed with CCE1 endonuclease appears to be general for all the junction-resolving enzymes that we have studied. We have shown this for T7 endonuclease I (Figure 6), as well as RusA (data not shown). Closer examination of time courses of junction cleavage by T4 endonuclease VII [see Figure 3C in Giraud-Panis and Lilley (*20*)] strongly suggests that this mechanism is correct for this enzyme too. Shah et al. (*34*) showed that the cleavages induced by RuvC could be uncoupled if one of the scissile phosphates was replaced by a 3′-*S*-phosphorothiolate.

CCE1 cleavage reactions were carried out under single-turnover conditions, i.e., the enzyme was present in a large excess over substrate and at a concentration where all the cruciform substrate should be bound by enzyme. We have analyzed the kinetic behavior of the cleavage reaction using the sequential model presented in Figure 7A. This assumes that either site can be cleaved first (with rate constants k_1 and k_2) to generate the nicked species as a transient intermediate, followed by the cleavage of the remaining site (with rate constants k_3 and k_4) to give the final linear DNA product. The linear differential equations corresponding to this mechanism were integrated by standard methods, leading to the following equations for the fraction of supercoiled, nicked and linear species as a function of time:

$$[S]_t/[S]_0 = e^{-(k_1+k_2)t} \quad (1)$$

$$[N]_t/[S]_0 = \frac{k_1}{k_1+k_2-k_3}[e^{-k_3t} - e^{-(k_1+k_2)t}] + \frac{k_2}{k_1+k_2-k_4}[e^{-k_4t} - e^{-(k_1+k_2)t}] \quad (2)$$

$$[L]_t/[S]_0 = 1 - e^{-(k_1+k_2)t} - \frac{k_1}{k_1+k_2-k_3}[e^{-k_3t} - e^{-(k_1+k_2)t}] - \frac{k_2}{k_1+k_2-k_4}[e^{-k_4t} - e^{-(k_1+k_2)t}] \quad (3)$$

where $[S]_t$, $[N]_t$, and $[L]_t$ are the concentrations of supercoiled, nicked, and linear species at time t, and $[S]_0$ is the concentration of supercoiled substrate at zero time. The best fits to the experimental data based on these equations are shown in Figure 7B. Fitting the data for the disappearance of supercoiled DNA by nonlinear regression to eq 1 (with a correction to allow for the small fraction of DNA that remained uncleaved at long times; this is probably DNA that has failed to extrude the cruciform) gave a value for (k_1 + k_2) of 0.027 ± 0.007 s^{-1}, where k_1 and k_2 are the rate constants for the cleavage at sites A and G, respectively. This is slightly lower than the sum of the rate constants for cleavage of the same sequences as isolated junctions, where k_1 = 0.03 s^{-1} and k_2 = 0.011 s^{-1} (*17*), which sum to 0.041 s^{-1}. This difference must reflect the lower efficiency of cleavage of the cruciform substrate, possibly for steric or topological reasons. For the analysis of the remaining kinetic data, we have assumed that k_1 and k_2 are in the same

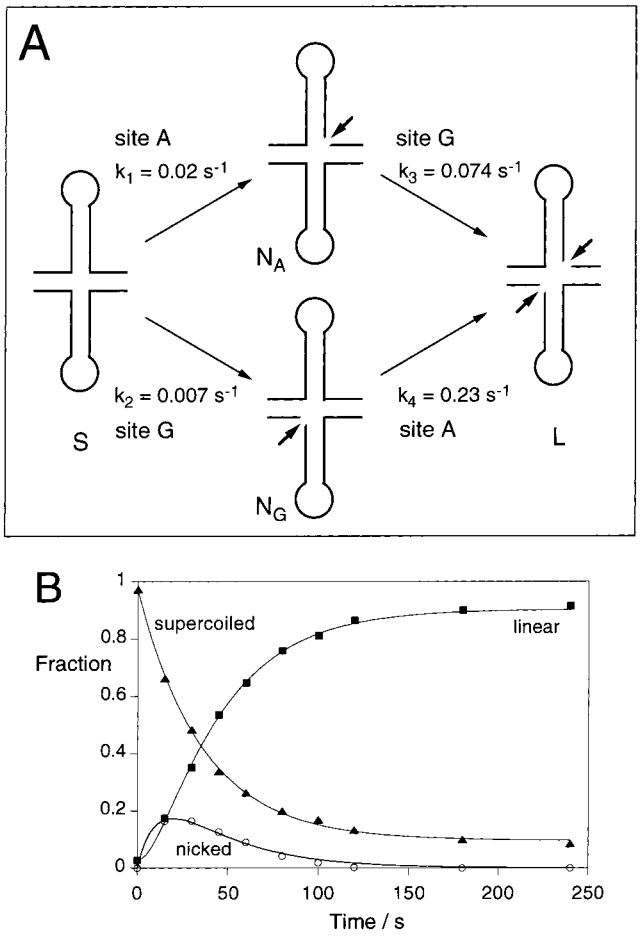

FIGURE 7: Kinetic model for the cleavage of a cruciform junction by CCE1. (A) The kinetic model used to analyze the data, and the calculated rate constants. This is based on a branched pathway. In the upper path, site A is cleaved initially with rate k_1 followed by site G (rate k_3). In the lower path, site G is cleaved first (rate k_2) followed by site A (rate k_4). The values of the rate constants were calculated by the fits to the experimental data. Note that k_4 and k_3 are 10-fold larger than k_1 and k_2, respectively, indicating that the rate of cleavage of a given site is accelerated once the first cleavage has been made. The species indicated are supercoiled DNA (S), linear DNA (L), and circular DNA nicked at the A (N_A) and G (N_G) sites, respectively. (B) Fits to CCE1 data using the branched kinetic model. The points show the fractions of supercoiled (▲), nicked (○), and linear (■) pCCE DNA measured experimentally at 37 °C. The fits were generated by nonlinear regression, using the integrated rate eqs 1−3 shown in the text.

proportion as the values measured previously for isolated junctions (*17*), and thus $k_1 = 0.020\ s^{-1}$ and $k_2 = 0.0074\ s^{-1}$. These values were applied to the analysis of the appearance and disappearance of nicked DNA (eq 2), and the appearance of linear DNA (eq 3). It might have been anticipated that the values $k_1 = k_4$ and $k_2 = k_3$, since the same sites are being cleaved (i.e., sites A and G respectively; see Figure 7). However, this requirement leads to a significant overestimation of the fraction of nicked circular DNA generated, and the values that best fitted the experimental data by nonlinear regression were $k_3 = 0.074\ s^{-1}$ and $k_4 = 0.228\ s^{-1}$. This reveals an acceleration of the subsequent cleavage reactions, by around 10-fold for both sites. We have found that the measured rate enhancement factor can vary between 5 and 10 for different preparations of enzyme. The nicked DNA contains a mixture of the two possible singly cleaved species, and at time *t*, the ratio of species cleaved at sites A and G ($F_{A/G}$) is given by

$$F_{A/G} = [N_A]_t/[N_G]_t = \left\{\frac{k_1}{k_1 + k_2 - k_3}[e^{-k_3 t} - e^{-(k_1+k_2)t}]\right\}/ \left\{\frac{k_2}{k_1 + k_2 - k_4}[e^{-k_4 t} - e^{-(k_1+k_2)t}]\right\} \quad (4)$$

where N_A and N_G are nicked species resulting from cleavage at sites A and G, respectively. After 20 s reaction, the proportion of nicked species is at a maximum. The $F_{A/G}$ ratio was calculated to be 1.7 in favor of site A at 30 s. This is in good agreement with the measured ratio (see above) of 1.9, assuming equal phosphorylation efficiencies for the two termini.

The result that clearly emerges from this kinetic analysis is that the CCE1 cleavage reaction is significantly faster for a given site when the other site has already been cleaved, i.e., the cleavage proceeds faster in the context of a nicked junction compared to one that is intact. A working model to account for this observation is as follows. On binding to a four-way junction, CCE1 greatly distorts both the global (*35*) and local (*36*) DNA structure. This suggests that the DNA structure is strained within the complex, which could hinder access to the active site of the enzyme. On cleavage of the first site, this strain might be relieved, such that the DNA is now better accommodated into the active site of the second protomer with a consequent increase in the rate of cleavage. This suggests that recognition and manipulation of DNA structure and the mechanism of cleavage are all intimately related and must, therefore. be studied as a whole. Some support for this idea can be taken from the studies of the Cre recombinase with a four-way DNA junction based on the *loxP* site (*37*). The DNA structure is clearly distorted in the complex, and the resulting lowered symmetry leads to a biased attack by Cre subunits.

From our measured kinetic constants we can estimate the lifetime of the enzyme−nicked junction complex. The slower rate for second cleavage has a rate constant $k_3 = 0.074\ s^{-1}$, which corresponds to a lifetime for the nicked intermediate of 14 s. However, the lifetime could potentially be considerably longer than this. In experiments using cruciforms with CCE1 cleavage sequences such that one site is cleaved more slowly, we have observed that the lifetime of the enzyme-nicked junction intermediate can be increased while retaining eventual complete conversion to linear product (data not shown). The retention of the complex with the nicked junction is important for the biological function. If a resolving enzyme were to dissociate from a Holliday junction after the first cleavage step, the DNA could branch migrate before reassociation resulting in the two cleavages being unopposed. The DNA would, therefore, remain as an unresolved junction containing single-stranded breaks in the arms. The enzyme must essentially freeze the structure of the junction, since branch migration of even a single step would reposition the cleavage site and thus seriously impede cleavage. The long lifetime of the frozen enzyme−junction complex together with the accelerated second cleavage step ensures bilateral cleavage, and thus a well-ordered resolution of the junction.

MATERIALS AND METHODS

Preparation of Supercoiled Plasmid DNA. The construction of pCCE is discussed in more detail in the Results. The

DNA was transformed into *E. coli* DH5α. The bacteria were grown to an $A_{660} = 0.6$, and the plasmid was amplified by treatment with 50 μg/mL chloramphenicol overnight. Plasmid DNA was isolated using the Wizard Maxiprep DNA purification kit (Promega) and purified by 2-fold isopycnic CsCl-ethidium bromide ultracentrifugation; supercoiled DNA was recovered by side puncture (*38*). Ethidium bromide was removed by extraction into *n*-butanol and the DNA subjected to extensive dialysis. This resulted in plasmid DNA comprising >95% negatively supercoiled circular DNA as determined by agarose gel electrophoresis. DNA concentrations were measured spectrophotometrically at 260 nm using an extinction coefficient of 6.5×10^{-3} M^{-1} cm^{-1} nt^{-1}. pCCE was characterized by means of restriction analysis using *Alw*NI, *Ase*I (New England Biolabs), and *Sty*I (Promega).

Expression and Purification of Junction Resolving Enzymes. CCE1. Wild-type CCE1 and the D294N mutant CCE1 were expressed and purified as described in (*35*). Briefly, *E. coli* BL21 (DE3) cells were grown at 28 °C with carbenicillin selection. Protein expression was induced with isopropyl β-D-thiogalactoside (IPTG) (0.05 mM), and the cells incubated for an additional 2.5 h. Cells were lysed by sonication, and the cleared lysate was subjected to ammonium sulfate fractionation. The CCE1-containing fraction was applied to a POROS HS 20/100 column (Perseptive Biosystems) and eluted with a gradient of 0.05 to 1.0 M NaCl. The peak fractions were concentrated and applied to a Superose-12 column (Pharmacia) and eluted isocratically. The purified CCE1 was analyzed by polyacrylamide gel electrophoresis in SDS-containing buffer and found to be approximately 95% homogeneous.

T7 Endonuclease I. This was expressed and purified as described previously (*33*). Briefly, BL21 (DE3) pLysS cells containing pET19*endoI* (*39*) were grown at 37 °C with carbenicillin selection. Protein expression was then induced by adding IPTG (1 mM), and the cells were further grown at 25 °C for 3 h. Frozen cell paste was thawed, resuspended in 50 mM sodium phosphate (pH 8), 200 mM NaCl, and lysed by sonication. Cleared supernatant was applied to a nickel chelating column (POROS 20 MC, Perseptive Biosystems) and T7 endonuclease I was eluted using an imidazole gradient. The eluate was >95% pure estimated polyacrylamide gel electrophoresis in SDS-containing buffer. Protein was finally concentrated using an Ultrafree centrifugal device (Millipore) and dialyzed against 20 mM Tris-HCl (pH 8), 1 mM EDTA, 1 mM DTT, and 50% glycerol.

CCE1 and T7 Endonuclease I Cleavage Reactions. Cleavage of Plasmid DNA by Different Concentrations of CCE1. Plasmid pCCE DNA (20 nM) was incubated with a range of concentrations of CCE1 in 20 mM Tris-HCl (pH 8.0), 200 mM NaCl, 0.1 mg/mL BSA, and 1 mM DTT (CCE1 reaction buffer) at 37 °C. $MgCl_2$ was added to a final concentration of 15 mM in a total reaction volume of 10 μL. The reactions were terminated after a fixed time by addition of 5 μL to a solution containing 250 mM EDTA and 1 mg/mL proteinase K and incubated for 20 min at 20 °C to digest any CCE1 still bound to the DNA before electrophoresis.

Time Course of the CCE1 Cleavage Reaction. pCCE DNA (20 nM) was incubated with 1 μM CCE1 in CCE1 reaction buffer at 37 °C. Reactions were initiated by addition of $MgCl_2$ to a final concentration of 15 mM in a volume of 50 μL. Aliquots of 5 μL were removed at intervals and added to a solution containing 250 mM EDTA and 1 mg/mL proteinase K and incubated for 20 min at 20 °C before electrophoresis.

Time Course of the T7 Endonuclease I Cleavage Reaction. pCCE DNA (40 nM) was preincubated in 50 mM Tris-HCl (pH 7.4), 50 mM NaCl, 0.1 mg/mL BSA, 1 mM DTT (endonuclease I reaction buffer) at 37 °C to ensure extrusion of the cruciform. T7 endonuclease I was then added to a final concentration of 500 nM and preincubated for a further minute to allow the enzyme to bind. The reaction mixture was then transferred to a 4 °C water bath and allowed to equilibrate to the new temperature before $MgCl_2$ was added to a final concentration of 10 mM in a volume of 50 μL. Aliquots of 5 μL were removed at intervals and treated as for the CCE1 cleavage reaction.

Cleavage Reactions with Heterodimeric CCE1. A range of mixtures of wild-type CCE1 and catalytically inactive D294N CCE1 giving a constant final concentration of wild-type enzyme (100 nM) with an increasing mole fraction of mutant enzyme were incubated together for 30 min at 20 °C to allow subunit exchange. After mixing DNA and enzyme in reaction buffer, $MgCl_2$ was added to a final concentration of 15 mM to give a total reaction volume of 10 μL. The samples were incubated at 37 °C for 10 min. Reactions were terminated by addition of 5 μL to a solution containing 250 mM EDTA and 1 mg/mL proteinase K and incubated for 20 min at 20 °C.

Analysis of Cleavage Products. Samples were loaded onto a 1% agarose gel and electrophoresed for 16 h at 30 V in 90 mM Tris·borate (pH 8.3) and 1 mM EDTA (TBE). DNA was stained using 1 μg/mL ethidium bromide and destained extensively in water. Gels were scanned using a FLA-2000 fluorescent image analyzer (Fuji) using excitation at 473 nm with an emission filter at 580 nm, and quantified using MacBas software (Fuji).

Quantitation of CCE1 Cleavages in the Nicked Intermediate Species. After electrophoretic separation, bands corresponding to the 30 s timepoint of a CCE1 time course reaction were excised from the agarose gel and the DNA isolated using a QIA extraction kit (Qiagen). 5′ Ends were dephosphorylated with calf alkaline phosphatase (Boehringer-Mannheim) and the DNA was precipitated with ethanol. The termini generated by CCE1 cleavage were radioactively 5′-^{32}P-labeled using T4 polynucleotide kinase, followed by complete digestion with the restriction enzymes *Ssp*I and *Sph*I (New England Biolabs). Samples were applied to a 6% denaturing polyacrylamide gel and electrophoresed in TBE buffer for approximately 2 h at 75 W. The gel was dried and visualized by phosphorimaging using a BAS-200 phosphorimager (Fuji).

Oligonucleotide Synthesis. Oligonucleotides were synthesized using β-cyanoethyl phosphoramidite chemistry (*40*, *41*) on a 394 DNA/RNA synthesizer (Applied Biosystems) and purified by electrophoresis in 12% polyacrylamide containing 7 M urea. DNA containing bands were excised, and the pure oligonucleotides electroeluted and recovered by ethanol precipitation.

ACKNOWLEDGMENT

We thank our colleagues Drs. M. White and M. Kvaratskhelia for valuable discussion.

REFERENCES

1. Holliday, R. (1964) *Genet. Res. 5*, 282−304.
2. Broker, T. R., and Lehman, I. R. (1971) *J. Mol. Biol. 60*, 131−149.
3. Orr-Weaver, T. L., Szostak, J. W., and Rothstein, R. J. (1981) *Proc. Natl. Acad. Sci. U.S.A. 78*, 6354−6358.
4. Potter, H., and Dressler, D. (1976) *Proc. Natl. Acad. Sci. U.S.A. 73*, 3000−3004.
5. Schwacha, A., and Kleckner, N. (1995) *Cell 83*, 783−791.
6. White, M. F., Giraud-Panis, M.-J. E., Pöhler, J. R. G., and Lilley, D. M. J. (1997) *J. Mol. Biol. 269*, 647−664.
7. Kemper, B., and Garabett, M. (1981) *Eur. J. Biochem. 115*, 123−131.
8. de Massey, B., Studier, F. W., Dorgai, L., Appelbaum, F., and Weisberg, R. A. (1984) *Cold Spring Harbor Symp. Quantum Biol. 49*, 715−726.
9. Connolly, B., Parsons, C. A., Benson, F. E., Dunderdale, H. J., Sharples, G. J., Lloyd, R. G., and West, S. C. (1991) *Proc. Natl. Acad. Sci. U.S.A. 88*, 6063−6067.
10. Iwasaki, H., Takahagi, M., Shiba, T., Nakata, A., and Shinagawa, H. (1991) *EMBO J. 10*, 4381−4389.
11. West, S. C., Parsons, C. A., and Picksley, S. M. (1987) *J. Biol. Chem. 262*, 12752−12758.
12. Symington, L., and Kolodner, R. (1985) *Proc. Natl. Acad. Sci. U.S.A. 82*, 7247−7251.
13. White, M. F., and Lilley, D. M. J. (1997) *Mol. Cell Biol. 17*, 6465−6471.
14. Elborough, K. M., and West, S. C. (1990) *EMBO J. 9*, 2931−2936.
15. Stuart, D., Ellison, K., Graham, K., and McFadden, G. (1992) *J. Virol. 66*, 1551−1563.
16. White, M. F., and Lilley, D. M. J. (1996) *J. Mol. Biol. 257*, 330−341.
17. Schofield, M. J., Lilley, D. M. J., and White, M. F. (1998) *Biochemistry 37*, 7733−7740.
18. Shah, R., Bennett, R. J., and West, S. C. (1994) *Cell 79*, 853−864.
19. Fogg, J. M., Schofield, M. J., White, M. F., and Lilley, D. M. J. (1999) *Biochemistry 38*, 11349−11358.
20. Giraud-Panis, M.-J. E., and Lilley, D. M. J. (1997) *EMBO J. 16*, 2528−2534.
21. Kleff, S., Kemper, B., and Sternglanz, R. (1992) *EMBO J. 11*, 699−704.
22. Ezekiel, U. R., and Zassenhaus, H. P. (1993) *Mol. Gen. Genet. 240*, 414−418.
23. Lockshon, D., Zweifel, S. G., Freeman-Cook, L. L., Lorimer, H. E., Brewer, B. J., and Fangman, W. L. (1995) *Cell 81*, 947−955.
24. Lilley, D. M. J. (1980) *Proc. Natl. Acad. Sci. U.S.A. 77*, 6468−6472.
25. Panayotatos, N., and Wells, R. D. (1981) *Nature 289*, 466−470.
26. Mizuuchi, K., Mizuuchi, M., and Gellert, M. (1982) *J. Mol. Biol. 156*, 229−243.
27. Mizuuchi, K., Kemper, B., Hays, J., and Weisberg, R. A. (1982) *Cell 29*, 357−365.
28. Lilley, D. M. J., and Kemper, B. (1984) *Cell 36*, 413−422.
29. Courey, A. J., and Wang, J. C. (1983) *Cell 33*, 817−829.
30. Lilley, D. M. J., and Hallam, L. R. (1984) *J. Mol. Biol. 180*, 179−200.
31. Greaves, D. R., Patient, R. K., and Lilley, D. M. J. (1985) *J. Mol. Biol. 185*, 461−478.
32. Murchie, A. I. H., and Lilley, D. M. J. (1987) *Nucleic Acids Res. 15*, 9641−9654.
33. Parkinson, M. J., and Lilley, D. M. J. (1997) *J. Mol. Biol. 270*, 169−178.
34. Shah, R., Cosstick, R., and West, S. C. (1997) *EMBO J. 16*, 1464−1472.
35. White, M. F., and Lilley, D. M. J. (1997) *J. Mol. Biol. 266*, 122−134.
36. Déclais, A.-C., and Lilley, D. M. J. (2000) *J. Mol. Biol. 296*, 421−433.
37. Guo, F., Gopaul, D. N., and Van Duyne, G. D. (1999) *Proc. Natl. Acad. Sci. U.S.A. 96*, 7143−7148.
38. Murchie, A. I. H., and Lilley, D. M. J. (1992) *Methods Enzymol. 211*, 158−180.
39. Duckett, D. R., Giraud-Panis, M.-E., and Lilley, D. M. J. (1995) *J. Mol. Biol. 246*, 95−107.
40. Beaucage, S. L., and Caruthers, M. H. (1981) *Tetrahedron Lett. 22*, 1859−1862.
41. Sinha, N. D., Biernat, J., McManus, J., and Koster, H. (1984) *Nucleic Acids Res. 12*, 4539−4557.

BI992785V